JOURNAL OF Materials CHEMISTRY

Modification of the interlayer pore structure of silica iron oxide sol pillared clay using organic templates

Yang-Su Han and Jin-Ho Choy*†

Department of Chemistry, Center for Molecular Catalysis, Seoul National University, Seoul 151–742, Korea

A novel route for modifying the interlayer pore structure of silica iron oxide sol particle pillared montmorillonite was proposed based on the post-intercalation of organic templates. The pristine mixed oxide sol pillared montmorillonite (SFM) was prepared by the reaction of Na-montmorillonite with silica iron sol particles obtained by depositing iron hydroxy cations on hydrolyzed silica sol surfaces. Three kinds of surfactant molecules with different molecular geometries and sizes were subsequently introduced between the interlayer spaces of the oxide sol exchanged montmorillonite. Upon intercalating the organic templates, a part of the interlayer sol particles was replaced and rearranged by the templates. Removing the templates by calcination at 550 °C resulted in the mesoporous sol pillared clays with controlled pore structures. The porous characteristics of the modified pillared clays were analyzed in detail using nitrogen and some selected solvent adsorption–desorption isotherms, which exhibited extremely large BET surface areas up to 750 $m^2\ g^{-1}$ and enlarged pore sizes of >20 Å.

In recent years, great attention has been paid to the layer silicate intercalation compounds cross-linked with inorganic or organic clusters, which are called pillared interlayered clays (PILCs) or cross-linked smectites (CLS).[1–4] These intercalation compounds may have a two-dimensional pore size larger than that of conventional zeolites and exhibit specific properties depending upon the nature of the pillars. PILC has attracted considerable interest as a new type of microporous solid due to its intrinsic catalytic activity, large surface area, thermal stability, and molecular sieving effect.

These materials are usually prepared by ion-exchanging the cations in the interlayer region of swelling clays with bulky organic cations, metal chelates, metal polyoxycations, and positively charged colloidal particles. The intercalated species are capable of preventing the collapse of the interlayer spaces, propping open the layers as pillars, and forming interlayer space, *i.e.*, a two-dimensional porous network. On heating, the intercalated inorganic species are converted into metal oxide clusters, generating a stable microporous structure. So far various kinds of metal oxides has been reported in the literature as pillars to keep the silicate layers apart.[5–23]

Most of the pillared clays reported, however, exhibit basal spacing less than 20 Å, corresponding to gallery heights of less than 10 Å. Thus, to improve upon the limited pore sizes available in metal oxide pillared clays, much effort has been paid to the new type of pillared clays with large pillar height, 'supergallery' pillared clays.[24–26] Because their pillar height is substantially larger than the host silicate layers (*ca.* 10 Å), they can provide pores of a larger size range, which, in turn, extend their applicability in the catalysts and shape-selective adsorbents to larger guest species.

In the previous report,[27] silica sol particles obtained by the hydrolysis of silicon tetraethoxide have been successfully intercalated into montmorillonite after modifying the surface with iron polyhydroxy cations. Thus prepared sol pillared clays exhibited extremely large basal spacings up to 60 Å, which can be called 'supergallery' pillared clays, and showed large BET specific surface areas (*ca.* 720 $m^2\ g^{-1}$) and excellent thermal stability at least up to *ca.* 800 °C. In spite of the large interlayer separation of the sol pillared clays, the pores obtained were mainly micropores with a dimension of *ca.* 10 Å due to the multilayer stacking of nanosize (1–2 nm) oxide sol particles between the silicate layers where the interstices between sol particles and silicate layers act as pores. This may be the reason why the dimension of the pores is not dependent on the interlayer separation.

It is of great importance, therefore, to explore new ways to fine-tune the interlayer pore textures in sol pillared clays to obtain tailor-made porous materials and to enhance the molecular sieving effect. One of the promising ways to meet this end involves the intercalation of organic templates into oxide sol exchanged clays.[28] Upon reacting the sol exchanged clays with bulky surfactant molecules such as quaternary alkylammoniums, a part of the sol particles would be replaced or rearranged by organic templates, and subsequent burning off the organics leaves behind large voids between the interlayer sol particles. The resulting pore textures, then, will strongly be correlated to the molecular geometry and volume of the templates, allowing the fine-tuning of porous textures.

In the present study, we describe a new synthetic route for mesoporous sol pillared clays by the post-intercalation of organic templates. Three kinds of surfactant molecules with different molecular geometry and volume were used as organic templates along with SiO_2–Fe_2O_3 oxide sol pillared clay. The adsorption properties and pore structures of the modified sol pillared clays are discussed in detail.

Experimental

Materials

The natural Na-montmorillonite (Kunipia G, Kunimine Industry, Japan) with the chemical formula of $Na_{0.35}K_{0.01}Ca_{0.02}(Si_{3.89}Al_{0.11})(Al_{1.60}Mg_{0.32}Fe_{0.08})O_{10}(OH)_2{\cdot}nH_2O$ and the cation exchange capacity (CEC) of 100 mequiv. (100 g^{-1}) was used as clays. An aqueous suspension (1 mass%) of the montmorillonite was prepared and pre-swelled for 24 h prior to ion exchange reaction.

Three kinds of alkylammonium surfactants, octadecylammonium chloride $[CH_3(CH_2)_{17}NH_3{}^+Cl^-]$, trimethylstearylammonium chloride $[CH_3(CH_2)_{17}N(CH_3)_3{}^+Cl^-]$, and distearlydimethylammonium chloride $[(CH_3(CH_2)_{17})_2N(CH_3)_2{}^+Cl^-]$ were used as received. These three compounds will be abbreviated hereafter as OD, MS and DS, respectively.

†E-mail:jhchoy@plaza.snu.ac.kr

Preparation

The pristine SiO_2–Fe_2O_3 sol pillared montmorillonite (SFM) was prepared as reported in elsewhere.[27] A silica sol solution was prepared by mixing silicon tetraethoxide (TEOS), $Si(OC_2H_5)_4$ (41.6 g), 2 M HCl (10 ml) and ethanol (12 ml) and hydrolyzing the solution at room temperature for 2 h with continuous stirring. A 0.25 mol dm^{-3} Fe^{3+} aqueous solution was prepared by dissolving the appropriate amount of $Fe(NO_3)_3 \cdot 9H_2O$ in deionized water. The silica sol solution and Fe^{3+} aqueous solution were then mixed in a 10:1 mole ratio. Then the pH of the mixed solution was adjusted to 2.7 ± 0.2 by adding slowly 0.2 M NaOH solution to facilitate the polymerization of Fe species on the silica sol surface. The mixed sol solution was added to clay suspension in a molar ratio of Si:Fe:CEC = 50:5:1 and reacted at 60 °C for 3 h. The product was then separated by centrifugation and washed with a mixed solution of ethanol and water (1:1, v:v) several times to remove the excess sols.

The washed product (*ca.* 1 g) was dispersed again in distilled water (250 ml) and each alkylammonium salt was added to the suspension in the mole ratio of [Organic]:Fe = 1:1. Further intercalation reaction of organic molecules was carried out at room temperature for 12 h, followed by centrifuging, washing and drying. Finally, the dried products were heated at 550 °C for 2 h under ambient atmosphere to burn-off the templates.

Characterization

X-Ray diffraction (XRD) patterns were obtained on the oriented samples using a diffractometer (SRA-M18XHF, MAC Science Co.) with graphite monochromatized Cu-Kα radiation ($\lambda = 1.5405$ Å). Thermogravimetry (TG)–differential thermal analysis (DTA) was performed on the dried samples with a heating rate of 5 °C min^{-1} and under a stream of oxygen and nitrogen gas of 1:1 volume ratio (flow rate = 100 ml min^{-1}).

Adsorption–desorption isotherms for nitrogen were measured volumetrically at the liquid nitrogen temperature by using a computer-controlled measurement system. The samples were degassed at 200 °C for 3 h under reduced pressure prior to the sorption measurement. Specific surface areas were estimated by using both BET and Langmuir equations and pore size distribution curves were calculated based on the adsorption branch of N_2 isotherms using the BJH method.[29] Adsorption–desorption isotherms for water and toluene vapors were measured gravimetrically at 25 °C by using a CAHN balance. The pillared samples were also degassed at 200 °C for 3 h prior to the sorption measurement.

Results and Discussion

Thermal analysis

Thermogravimetry (TG) and differential thermal analysis (DTA) curves of MS-modified sample are shown in Fig. 1 as an illustration. Three major steps for weight loss are observed in the TG curve. The first occurs up to 150 °C with a weak endothermic peak in the DTA curve. This step is assigned to the loss of surface physisorbed water and loosely coordinated water. The second step occurs between 150 and 350 °C with an intense exothermic peak corresponding to the oxidative decomposition of the organics. The weight loss observed in this stage was used to estimate the contents of organic molecules taken up by sol pillared samples, which are summarized in Table 1. An additional weight loss due to the dehydroxylation of silicate layers of the clays appears near 570 °C.

X-Ray diffraction

Fig. 2 shows the X-ray diffraction profiles of the pristine SFM (a) and modified samples [(b)–(d)] obtained after calcining at

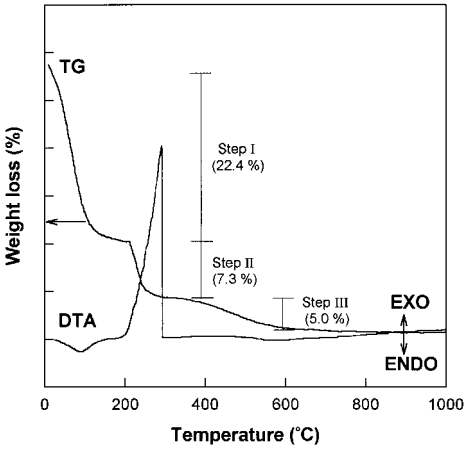

Fig. 1 TG–DTA curves of the SFM-MS sample dried at room temperature

550 °C for 2 h. As can be seen from Fig. 2(a), the pillaring of SiO_2–Fe_2O_3 sol particles expands the silicate layers as large as 58 Å, to form a 'supergallery' pillared clay. The second order reflection is also observed clearly, suggesting that the sol pillared clays are stacked in an ordered manner. Upon modifying with organic molecules [Fig. 2(b)–(d)], the basal spacings decrease from 58 Å to 40–44 Å and the diffraction lines are broadened, indicating that the rearrangement of interlayer sol particles takes place during the post-intercalation of organic templates. The decrease of the basal spacings might be originated from the difference between the gallery height of the pristine SFM and the molecular length of templates. The gallery height of SFM, after subtracting the layer thickness of montmorillonite (9.6 Å), is *ca.* 48 Å while the molecular lengths of organic templates used in this study are in the order of *ca.* 30 Å. Thus, the lengths of organic templates are insufficient to cover the full width of the interlayer distance even though the organic molecules are arranged perpendicularly between silicate layers. The broadening of diffraction profiles and the absence of higher order diffraction peaks for the modified samples suggests that the regular stacking of sol particles between the silicate layers and the long range ordering of platelet clay particles are destroyed partially with the incorporation of organic molecules. Even though, as yet, the exact origin of this behavior has not been elucidated, it is likely that the strong affinity of organic cations onto the negatively charged silicate surfaces causes, in part, the irregular stacking of clay platelets such as edge-to-face combination, which leads to a turbostatic stacking of clay particles after removing organic templates.

Nitrogen adsorption–desorption isotherms

Fig. 3 represents the nitrogen adsorption–desorption isotherms for the samples calcined at 550 °C. The adsorption isotherm of the pristine SFM(a) can be classified into the Type I in the BDDT classification,[30] which is characteristic of nitrogen adsorption on microporous adsorbents. This indicates that most of the pores formed in SFM are micropores. The hysteresis loops resemble H4 in the IUPAC classification,[30] which is attributable to the adsorbents having slit-shaped pores between parallel layers. The adsorption isotherm gives a good fit on the Langmuir (Type I) as well as BET equation even though a better fit is obtained on the BET equation for the limited number of nitrogen adsorption layers.

The modified samples [Fig. 3(b)–(d)] show characteristic adsorption–desorption behaviors depending upon the organic templates. Overall features of the isotherms can be characterized to an enhanced mesoporosity reflected by a steep increase at higher P/P_0 region during adsorption and an

Table 1 Specific surface areas and pore volumes of the pristine and modified silica iron oxide sol pillared clays calcined at 550 °C for 2 h

sample identification	amount of adsorbed organics (x)[a]	specific surface area/$m^2\ g^{-1}$		pore volume/ml g^{-1}
		BET	Langmuir	
SFM	—	540	900	0.39
SFM-OD	0.54	767	1345	1.45
SFM-MS	0.30	705	1157	0.63
SFM-DS	0.24	752	1238	0.84

[a]Calculated from the thermogravimetric (TG) analysis based on the formula of $[ORG]_x[(SiO_2)_{6.85}(Fe_2O_5)_{0.79}][(Si_{3.89}Al_{0.11})(Al_{1.60}Mg_{0.32}Fe_{0.08}]O_{10}(OH)_2$.

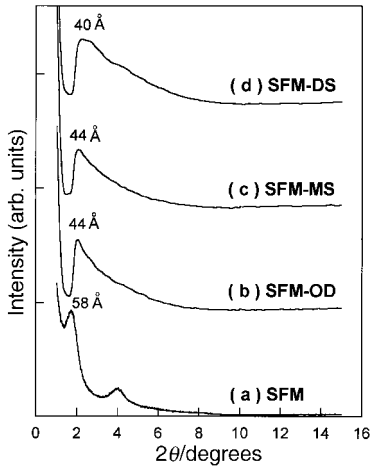

Fig. 2 X-Ray diffraction profiles of the pristine SFM (a) and the organically modified samples obtained after calcining at 550 °C for 2 h; (b) SFM-OD, (c) SFM-MS and (d) SFM-DS, respectively

enlarged hysteresis during desorption. The former is attributable to the capillary condensation of nitrogen molecules in mesopores. The mesoporosity of the modified samples increases in the order of MS < DS < OD. It is interesting to note here that the OD-modified sample exhibits the largest mesoporosity even though OD molecule has the smallest molecular volume. Another characteristic feature of the OD-modified samples (b) is a narrow hysteresis curve, indicating the pores in the SFM-OD sample must be very open and have ink-bottle type necks.[30]

The specific surface areas calculated from nitrogen adsorption isotherms by applying the BET and Langmuir equations are summarized in Table 1. Remarkably high BET specific surface areas up to 770 $m^2\ g^{-1}$ and pore volumes as large as 1.45 ml g^{-1} are observed after modification. It is worthy to note here that the samples calcined at 700 °C maintain fairly high BET specific surface area of $>600\ m^2\ g^{-1}$, indicating their high thermal stability. The adsorption isotherms of organic-modified pillared clays are well fitted by the BET equation rather than the Langmuir one, suggesting that the pore sizes are enlarged.

The pore size distribution curves of the pristine SFM and the modified samples are plotted in Fig. 4. These distribution curves are calculated by the BJH method[30] using the adsorption branches in Fig. 3. The pristine SFM mainly consists of micropores with the size of *ca.* 10 Å. Upon modifying, the pore volumes are increased in the domain of supermicropores or mesopores ranging from 15–60 Å. Averaged pore sizes of the modified samples increase in the order of MS < DS < OD. As mentioned before, OD-modified sample (b) has the largest pore size even though its molecular volume is the smallest among the organic templates used. This implies that the variation of pore size is not strictly consistent with the molecular dimension of the template.

Water adsorption–desorption isotherms

The adsorption–desorption isotherms for water are plotted in Fig. 5. The adsorption of water on the pristine SFM (a) is strongly suppressed in the low relative vapor pressure which is mainly attributed to the hydrophobicity developed on the pore surfaces after calcination.[27,31] However, once a water adsorption layer is formed, the stronger adsorbate–adsorbate interaction between water molecules will enhance further adsorption, which resulted in the linear increase at higher P/P_0. A similar adsorption behavior is also observed in the case of MS-modified sample (c). The adsorption isotherms of the OD-(b) and DS-(d) modified samples are of Type II in the

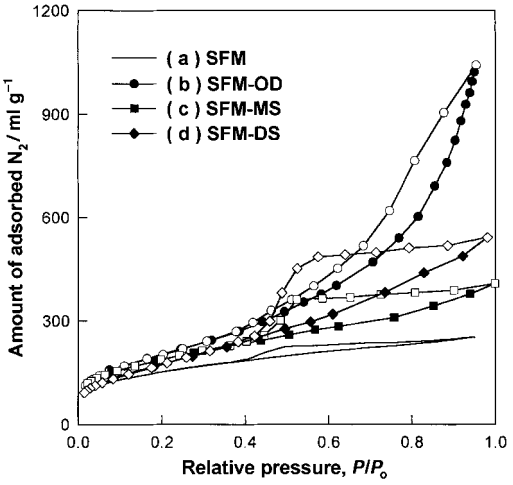

Fig. 3 Nitrogen adsorption (open symbols)–desorption (filled symbols) isotherms for the pristine SFM (a) and the organically modified samples calcined at 550 °C for 2 h; (b) SFM-OD, (c) SFM-MS and (d) SFM-DS, respectively

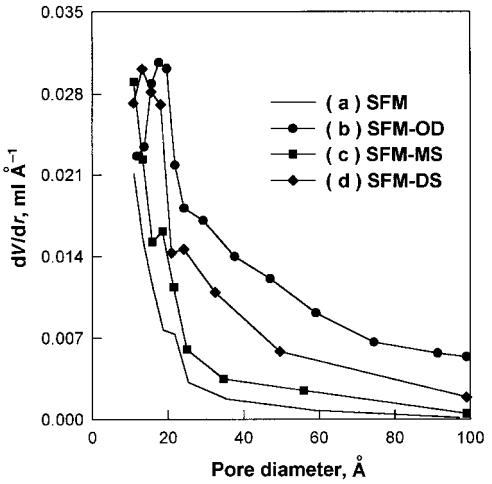

Fig. 4 Pore size distribution curves for the pristine SFM and the organically modified samples calcined at 550 °C for 2 h; (b) SFM-OD, (c) SFM-MS and (d) SFM-DS, respectively

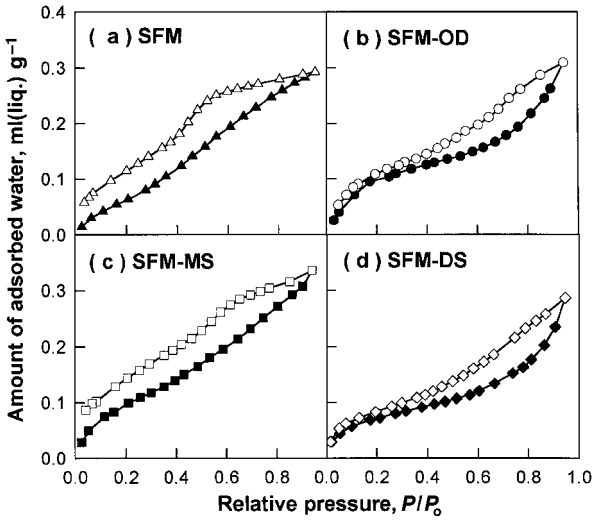

Fig. 5 Water adsorption–desorption isotherms for the pristine SFM (a), SFM-OD (b), SFM-MS (c) and SFM-DS (d), respectively, measured at 25 °C

BDDT classification.[30] This type of isotherm is the result of unrestricted monolayer–multilayer adsorption on a free, or on a quasi-free surface in widely opened pores. Thus, the slightly enhanced water uptake in the samples at lower P/P_0 might be due to the enlarged pore sizes.

All the isotherms exhibit large hysteresis during desorption extending to very low P/P_0, which is attributable to the rehydroxylation of silicate or pillar surfaces.[31] Rehydroxylation probably commences with physical adsorption, initiated by hydrogen bonding of water molecules to any remaining hydroxyl groups in the surfaces, which will produce low-pressure hysteresis. According to Fig. 5, the pore volumes measured by water adsorption are not consistent with those determined by nitrogen adsorption, which deviates from the Gurvitsch rule in the mesoporous solids.[30] Even though the exact origin for this has not been elucidated yet, the hydrophobicity of the pillar surface and the specific interaction between the pillar surface and water molecules seem to play an important role in adsorbing water molecules.

Toluene adsorption–desorption isotherms

The adsorption–desorption isotherms (A) and the BET and Langmuir plots for the corresponding isotherms (B) are shown in Fig. 6. The toluene adsorption on pristine SFM (a) follows the Langmuir type, indicating the multilayer adsorption of toluene molecules on the micropores is restricted due to the limited pore size. By modifying with organic templates, however, the adsorption behavior changed drastically depending upon the templates. In case of SFM-MS (c), the isotherm shape is very similar to that of the pristine SFM (a) though the adsorption capacity is almost doubled. The adsorption isotherm fits well with the BET as well as the Langmuir equation, reflecting that the adsorption of toluene occurs in the manner of a restricted multilayer. In addition, the desorption branch exhibits large hysteresis extending to low vapor pressure owing to the activated entry of toluene molecules into relatively small pores.[27] The adsorption isotherms of OD- (b) and DS- (d) modified samples fit well the BET equation rather than the Langmuir one, implying the multilayer adsorption of toluene molecules becomes possible owing to the increased pore dimension. Moreover, the adsorbed amount of toluene increases almost linearly and the hysteresis of desorption branches is weakened remarkably. The linear increase means that the primary adsorption process can be regarded as monolayer coverage in widely open pores rather than pore filling in micropores [for example the pristine SFM (a)]. The depressed hysteresis means a reduced activated entry of toluene molecules into restricted pores, which also suggests that the SFM-OD and -DS are mainly composed of opened pores.

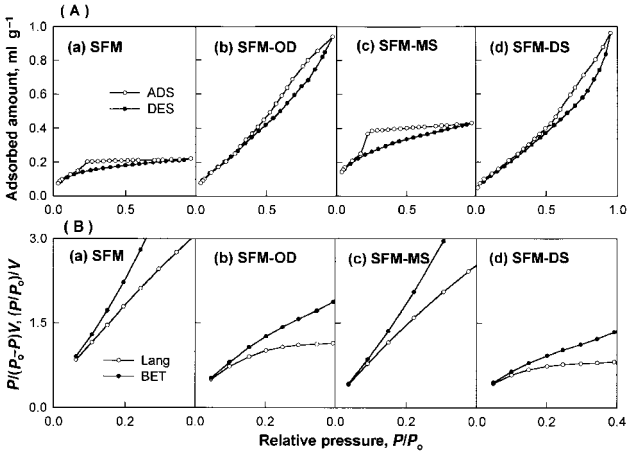

Fig. 6 Toluene adsorption–desorption isotherms (A) and the corresponding BET and Langmuir plots (B) for the pristine SFM (a), SFM-OD (b), SFM-MS (c) and SFM-DS (d), respectively, measured at 25 °C

Mechanism for the modification of interlayer pore structure

An overall scheme for the modification of interlayer pore structures of SiO_2-Fe_2O_3 sol pillared clays by post-intercalation organic templates is shown in Fig. 7. Fe-modified silica sol particles, $Fe_x(OH)_y$–SiO_2, are easily introduced into the interlayer spaces of clays by ion exchange with Na^+ ions, to form a 'supergallery' pillared clay (b). In spite of its large interlayer separation of *ca.* 48 Å [Fig. 2 (a)], the adsorption data strongly suggest the presence of micropores (Fig. 3, 4 and 6), allowing us to propose the multilayer stacking of interlayer sol particles where the interstices between sol particles and silicate layers act as micropores.[27] Subsequent intercalation of organic templates into the SiO_2–Fe_2O_3 exchanged montmorillonite gives rise to a partial replacement and rearrangement of interlayer sol particles (c). Finally, the removal of organic templates by calcination leaves the pores with different sizes and shapes depending upon the templates used.

The porous texture of the modified samples seems to be regulated by not only the organic content intercalated but also the molecular geometry. The mole content of organics intercalated is increased in the order of OD > > MS > DS. Taking into account of molecular structures, it is quite acceptable. The OD molecules having a long alkyl chain group are intercalated easily and rapidly by replacing and rearranging the interlayer sol particles. The MS and DS molecules containing bulky head groups must be subjected to strong steric

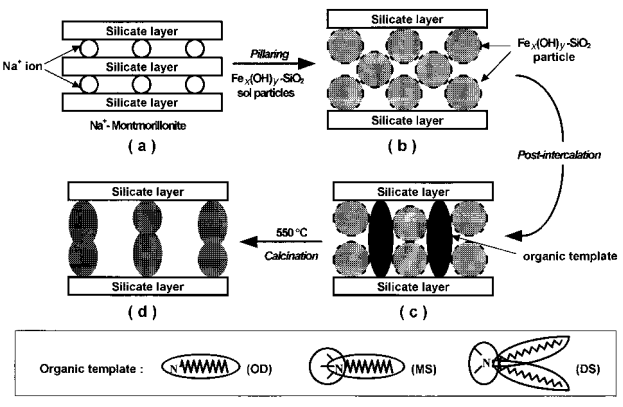

Fig. 7 Schematic model for the formation of mesoporous silica iron sol pillared clays

hindrance during intercalation. Moreover, the DS molecule having an extra long chain alkyl group would undergo strongest steric replusion, which limits the content of the organic templates between the layers.

According to the adsorption data (Fig. 3, 4, 6 and Table 1), the OD-modified sample exhibits the largest pore volume and pore size even though the OD molecule has the smallest molecular dimension. It is likely that the intercalated OD molecules form molecular aggregates of two or three OD molecules through the van der Waals attraction between alkyl chains, leaving behind the mesopores between the layers after removing the templates. MS molecules are also inserted into interlayer space modifying the arrangement of interlayer sol particles. However, the presence of the bulky head group limits the organic content, resulting in the minor interspace modification. Even though the interlayer content of DS molecules is also restricted, even more severely than MS molecules, owing to the large steric hindrance, the incorporation of DS molecules exerts a great influence on the modification of interlayer space owing to their large molecular volume.

Conclusions

New mesoporous silica iron sol pillared clays were prepared by the post-intercalation of bulky organic templates into silica iron sol pillared clay. The post-intercalation of bulky organic cations with different molecular geometry and volume gave rise to the rearrangement of interlayer sol particles, resulting in mesoporous sol pillared clays with controlled pore structures after burning off the organics. The mesoporous pillared materials obtained here exhibited remarkably high BET surface areas and pore volumes up to $760\ m^2\ g^{-1}$ and $1.45\ ml\ g^{-1}$, respectively. The porous textures of the modified samples seemed to be regulated by not only the organic content intercalated but also the molecular geometry of the templates.

We wish to thank Professor Shoji Yamanaka of Hiroshima University for his helpful discussions and for providing research facilities. This work was in part supported by KOSEF through the Center for Molecular Catalysis.

References

1 R. M. Barrer, *Zeolites and Clay Minerals as Sorbents and Molecular Sieves,* Academic Press, New York, 1978, ch. 8.
2 T. J. Pinnavaia, *Science,* 1983, **220**, 365.
3 *Pillared Clays*; *Catalysis Today*, ed. R. Burch, Elsevier, New York, 1988, vol.2 no.2–3.
4 F. Figueras, *Catal. Rev.-Sci. Eng*., 1988, **30**, 457.
5 G. W. Brindley and R. E. Sempels, *Clay Miner*., 1977, **12**, 229.
6 S. Yamanaka and G. W. Brindley, *Clays Clay Miner*., 1979, **27**, 119.
7 T. Endo, M. M. Mortland and T. J. Pinnavaia, *Clays Clay Miner*., 1980, **28**, 105.
8 M. L. Occelli and D. H. Pinseth, *J. Catal*., 1986, **99**, 316.
9 D. Plee, F. Borg, L. Gatineau and J. J. Fripiat, *J. Am. Chem. Soc*., 1985, **107**, 2362.
10 T. J. Pinnavaia, M. S. Tzou, S. D. Landau and I. D. Johnson, *J. Am. Chem. Soc*., 1985, **107**, 7222.
11 S. Yamanaka, T. Doi, S. Sako and M. Hattori, *Mater. Res. Bull*., 1984, **19**, 161.
12 M. L. Occelli, *J. Mol. Catal*., 1986, **35**, 377.
13 S. Yamanaka, S. Nishihara and M. Hattori, *Mater. Chem. Phys*., 1987, **17**, 87.
14 A. Drljaca, J. R. Anderson, L. Spiccia and T. W. Turney, *Inorg. Chem*., 1992, **31**, 4894.
15 F. González, C. Pesquera, C. Blanco, I. Benito and S. Mendioroz, *Inorg. Chem*., 1992, **31**, 727.
16 K. Ohtsuka, Y. Hayashi and M. Suda, *Chem. Mater*., 1993, **5**, 1823.
17 X. Tang, W. Q. Xu, Y. F. Shen and S. L. Suib, *Chem. Mater*., 1995, **7**, 102.
18 A. Gil, G. Guiu, P. Grange and M. Montes, *J. Phys. Chem*., 1995, **99**, 301.
19 J. Bovey and W. Jones, *J. Mater. Chem*., 1995, **5**, 2027.
20 E. Booij, T. Kloprogge and J. A. Rob van Veen, *Clays Clay Miner*., 1996, **44**, 774.
21 M. J. Hernando, C. Pesquera, C. Blanco, I. Benito and F. González, *Chem. Mater*., 1996, **8**, 76.
22 S. Moreno, R. Sun Kou and G. Poncelet, *J. Phys. Chem. B*, 1997, **101**, 1569.
23 I. Palinko, A. Molnar, J. B. Nagy, J-C. Bertrand, K. Lazar, J. Valyon and I. Kiricsi, *J. Chem. Soc*., *Faraday. Trans*., 1997, **93**, 1591.
24 A. Moni and T. J. Pinnavaia, *Solid State Ionics*, 1988, **26**, 119.
25 J. Guan and T. J. Pinnavaia, *Mater. Sci. Forum*, 1994, **152–153**, 109.
26 S. Yamanaka, Y. Inoue, M. Hattori, F. Okumura and M. Yoshikawa, *Bull. Chem. Soc. Jpn*., 1992, **65**, 2494.
27 Y. S. Han, H. Matsumoto and S. Yamanaka, *Chem. Mater*., 1997, **9**, 2013.
28 K. Takahama, M. Yokoyama, M. Hirao, S. Yamanaka and M. Hattori, *J. Ceram. Soc. Jpn*., 1991, **99**, 14.
29 E. P. Barrett, L. G. Joyner and P. P. Halenda, *J. Am. Chem. Soc*., 1951, **73**, 373.
30 S. J. Gregg and K. S. W. Sing, *Adsorption, Surface Area and Porosity*, Academic Press, London, 1982.
31 S. Yamanaka, P. B. Malla and S. Komarneni, *J. Colloid. Interface Sci*., 1990, **134**, 51.

Paper 8/00228B; *Received* 7*th January*, 1998